

# CHALMERS



## Physical modeling of a clutch for heavy vehicles

*Master of Science Thesis*

LISA WESSLING

Department of Signals and Systems  
*Division of Automatic Control, Automation and Mechatronics*  
CHALMERS UNIVERSITY OF TECHNOLOGY  
Göteborg, Sweden, 2011  
Report No. EX019/2011



Thesis for the degree of Master of Science in Systems, Control and  
Mechatronics

# Physical modeling of a clutch for heavy vehicles

---

**Lisa Wessling**

Department of Signals and Systems  
Chalmers University of Technology

February 2011



I've always seen modeling as a stepping stone.

Tyra Banks (1973 - )



# Physical modeling of a clutch for heavy vehicles

Lisa Wessling  
Department of Signals and Systems  
Chalmers University of Technology  
SE-412 96 Göteborg, Sweden

## Abstract

The development of a new truck starts at the desk of a construction engineer. Yesterday's slide-rules have been replaced by today's computerised simulations that are used in the process when evaluating control functions as well as physical components before the truck is produced for real. This puts great demand on the models representing each component in terms of accuracy and quality.

The aim of this master thesis, accomplished on behalf of Volvo Powertrain Corporation, was to increase the knowledge of the function of a single clutch by setting up an analytical clutch model. Through a theoretical clutch model it is anticipated that further development of the clutch can be facilitated. The purpose was to formulate and derive mathematical and physical formulas for the clutch movement and function.

The modeling process consists of three separate phases. The first one is the structural phase where it is important to understand the function of the system to be able to divide it into subsystems. In the second phase variables and constants are identified and the relationships that combine them are set up. In the third and last phase the derived model is implemented in a simulation program where it is tested and evaluated.

The results from simulation tests show that the analytical model behaves as expected. It is accurate even though several simplifications were needed due to the complexity of the system. However it may be possible to improve its accuracy even further if closer studies of for example the clutch disc surface could be carried out.





## **Acknowledgement**

First of all I would like to thank my examiner and Chalmers Professor Bo Egardt for his positive and realistic mindset during particularly difficult project states. Another Chalmers employee of significant importance during the project is Gunnar Johansson, Department of Fluid mechanics. His enthusiasm and experience, combined with his constant positive mindset and encouraging spirit has been a guiding light to say the least.

I would also like to direct a special thanks to my supervisor at Volvo Powertrain, Andreas Magnusson; my enduring desk buddy Henrik Ryberg; the technical oracle Erik Lauri; the hardware experts Sami Aho and Lars Zetterstrand; and the Transmission function group at Volvo Powertrain for including me in their group community welcoming me from day One.

Last, but far more than least, the support from my husband has been invaluable. Thank you for all the late night hypothetical discussions as well as limitless support during ups and downs during the project. In fact, throughout all my years at Chalmers.

Göteborg, February 2011



# Contents

<b>1</b>	<b>Introduction</b>	<b>1</b>
1.1	Purpose . . . . .	2
<b>2</b>	<b>Method</b>	<b>3</b>
2.1	A physical modeling process . . . . .	3
2.2	Function of a clutch . . . . .	3
<b>3</b>	<b>The clutch system - An analytical approach</b>	<b>5</b>
3.1	Structuring the system . . . . .	5
3.2	Part I - Air in and out of the clutch system . . . . .	6
3.2.1	Clutch valve unit . . . . .	7
3.2.2	Clutch Concentric Actuator . . . . .	10
3.2.3	Gas dynamics . . . . .	10
3.2.4	Air flow in and out of CCA . . . . .	12
3.2.5	Piston movement . . . . .	13
3.3	Part II - Force on Clutch plate . . . . .	14
3.3.1	Diaphragm spring and Clutch plate . . . . .	15
3.4	Part III - Transferred torque . . . . .	16
3.4.1	Friction, radius and wear . . . . .	16
3.5	Formulation of the complete model . . . . .	17
3.6	Simulation Model . . . . .	19
<b>4</b>	<b>Results</b>	<b>21</b>

4.1	Model behavior . . . . .	22
4.2	Valve tests in test bench . . . . .	22
4.3	In vehicle test . . . . .	24
4.4	Drive line rig test . . . . .	25
<b>5</b>	<b>Discussion and conclusions</b>	<b>27</b>
5.1	Uncertainties . . . . .	30
5.2	Final conclusions . . . . .	30
<b>6</b>	<b>Future work</b>	<b>33</b>

# 1

## Introduction

The development of next generation's heavy vehicle starts in general at the desk of a constructing engineer. More specifically at hers/his computer. It is a process stretching over several years which includes hundreds of people. Each and every one working on their piece in this huge puzzle that later becomes a truck. At Volvo Powertrain, Gothenburg, the driveline of heavy vehicles is constructed. In order to predict the performance of the driveline several simulations are carried out long before the truck is built for real in the production line. This makes it important to have realistic models that reflect mechanical components as well as functions.

In recent years, the behaviour and performance of a heavy vehicle is optimized in a computerized environment through the introduction of complex control strategies and algorithms. Parameters and software is validated in a simulated milieu which sets high demand on the models representing different parts such as the engine, clutch and gearbox. For this specific master thesis the model of the clutch is subject for further development.

The clutch models that are used at present are based on test results from empirical studies. The collected data are implemented in the models through the simple "black box"-principle, i.e.  $x$  goes in and  $y$  comes out. These estimations may imply unnecessary large control error when parameters are changed. In order to diminish the uncertainty a more accurate model is of interest. If implemented in a simulation and validated as close enough to generated test data the model might be a useful tool for further development of the clutch.

## 1.1 Purpose

The overarching purpose of this master thesis is to present an analytical model that can contribute to a greater understanding of the clutch and its function. The main reason to why this is found important is that, as an extension, this knowledge is the essence for facilitation of further development of the clutch. With an improved clutch model functionality can be tested in a simulated environment which is far more time efficient and economically sustainable than if *real* physical clutch models are used. To specify the purpose further: a dynamic model of the clutch for heavy vehicles is to be derived in an analytical manner with a physical approach. It will not include any other control algorithms or constraints other than what is implied by mechanical, physical and/or mathematical theory. The input signals to the system are the ones that control the physical clutch movement. From these in signals the model treat the dynamic course of events that end with an ingoing torque to the gearbox. Through simulations the model is tested and evaluated.

When the analytical model is formulated it is built in MATLAB-Simulink. In order to validate the new model, simulated results are compared to test data drawn from, for example, in vehicle tests. In an attempt to move away from the dependence on empirical data the model shall, to the extent it is possible, rely on mathematical formulas and physical theorems. Due to this the physical characteristics of the separate components that the clutch consist of needs to be taken into thorough consideration.

# 2

## Method

### 2.1 A physical modeling process

The purpose, as stated in Chapter 1 is to formulate an analytical clutch model that represents the clutch behavior. The method used for the modeling process is the one presented by [3] where the three different modeling phases are identified.

**Phase 1** First of all the system is broken down into smaller parts, subsystems, to achieve structure. To be able to decide how this breakdown is most efficiently done a good understanding of the system is important.

**Phase 2** Each block is studied closely and basic formulas that represent relationships between variables and constants are formulated. In order to do so assumptions and simplifications are not unlikely needed.

**Phase 3** The equations formulated previously in phase 2 are structured into state space models. This phase can be viewed upon as a summary of the whole system that now is ready to be implemented in a computerized environment where its behavior and accuracy can be tested. For this thesis work MATLAB-Simulink is used.

### 2.2 Function of a clutch

The clutch in a driveline connects engine with gearbox and is thus of essential importance for the movement of the vehicle, see Figure 2.1. The main functions of the clutch are:

- transfer torque and movement from engine to transmission

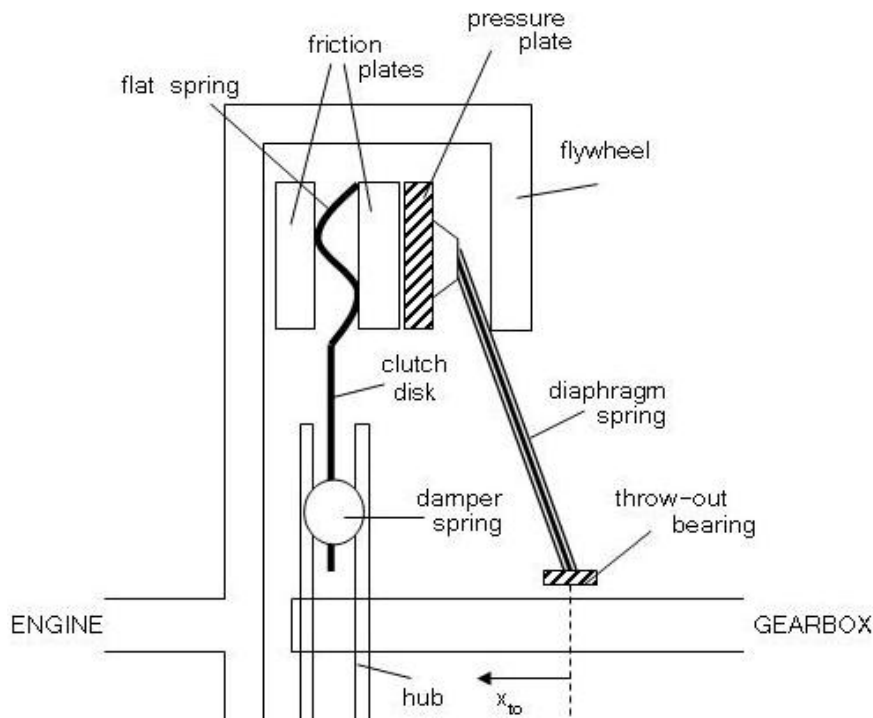


**Figure 2.1:** A simplified figure of the components that make up the clutch.  $x_{to}$  is the throw-out bearing position. When the throw-out bearing is moved in the direction indicated by the arrow the pressure plate in the other end of the diaphragm spring will ease its pressure on the friction plates and so the clutch is disengaged.

- damp torque oscillations from engine
- make it possible to disengage the engine from driveline

The clutch consists of many mechanical components that through controlled movement operate together. The main function as stated is to disconnect/connect the flywheel mounted on the engine with the gear box input shaft. When these two are rotating with the same angular velocity the clutch is engaged. Different angular velocities on the other hand occur when the clutch is either completely disengaged or slipping; i.e. when the clutch is somewhere between engaged and/or disengaged.

A disconnection of the flywheel to the clutch plate is caused by a translational movement of the throw-out bearing, in Figure 2.1 indicated by the arrow  $x_{to}$ . Due to the diaphragm spring characteristics a movement of the throw-out bearing in this direction decrease the force acting on the pressure plate. The throw-out bearing position depends on the air pressure in the Clutch Concentric Actuator (CCA). The air pressure, in turn, is controlled by in- and outlet of air through four valves.



# 3

## The clutch system - An analytical approach

To structure the modeling process of the clutch as well as its function in a distinct way the problem is divided into subsystems (Section 3.1). Each part is individually described in detail and the analytical equations and mechanical relations used in the simulation model are derived (Section 3.2-3.4). These equations are structured (Section 3.5) and finally implemented in MATLAB-Simulink (Section 3.6).

### 3.1 Structuring the system

In an attempt to concretise the clutch and its function the modeling problem is divided into three different parts (see Figure 3.1):

**Part I** - from PWM-signals to throw-out bearing position

What causes the engagement/disengagement of the clutch is the *translational*



**Figure 3.1:** How the clutch system is divided and structured into three parts.

*movement* of the *throw-out bearing*. This movement in turn is caused by the *airpressure* in the CCA,  $P_{CCA}$ . The signals that control the opening and closing of the air valves that let air in or out of the CCA are the *PWM-signals*. Also, the *valve characteristics* are of importance when estimating the correct magnitude of the air mass flow. Another factor of importance when estimating the air mass flow is the already mentioned air pressure in the CCA since the flow will decrease with increasing pressure.

**Part II** - from throw-out bearing position to force on the clutch plate

For every throw-out bearing position,  $x_{to}$ , a force from the compressed *diaphragm spring* is exerted on the bearing,  $F(x)$ . The output from Part II is the spring's corresponding *force on the clutch plate*,  $F_{cp}$ , from the outer ring.  $F_{cp}$  is affected by the elastic characteristic in the clutch plate.

**Part III** - from force on clutch plate to torque on transmission shaft

The force on the clutch plate ( $F_{cp}$ ), and henceforth the torque transmitted to the gearbox shaft ( $T_{gbx}$ ), is for example affected by the friction coefficient  $\mu$ ; the wear of the clutch plate; and the clutch disc inner and outer radius ( $R_i$  and  $R_o$ ).

## 3.2 Part I - Air in and out of the clutch system

### Inputs:

$s_d, f_d, s_e, f_e$ : PWM-signals (%)

### Output:

$x_{to}$ : throw-out bearing position (mm)

### Internal variables:

$P_{CCA}$ : air pressure in CCA (Pa)

$\rho$ : air density in CCA ( $\text{kg/m}^3$ )

$V_{CCA}$ : CCA volume ( $\text{m}^3$ )

$\dot{m}_{in}$ : air mass flow into system (kg/s)

$\dot{m}_{out}$ : air mass flow out of system (kg/s)

$m_{tot}$ : total air mass in CCA (kg)

$F(x)$ : force from diaphragm spring (N)

### Constants:

$P_{airtank}$ : feed pressure (Pa)

$P_{atm}$ : atmospheric pressure (Pa)

$m_0$ : air mass in CCA from start (kg)

$A_{CCA}$ : piston cross sectional area ( $\text{m}^2$ )

$L_0$ : length of CCA from start (m)

$m_s$ : mass of moving parts in system i.e. piston, throw-out bearing (kg)

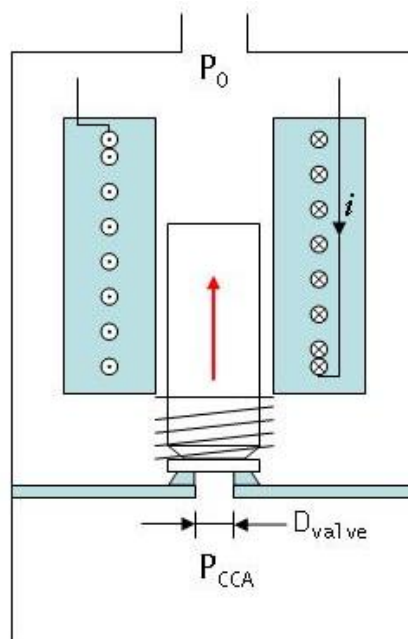


**Figure 3.2:** A current  $i$  induce a magnetic field that makes the valve move in the direction indicated by the arrow.

T: air temperature (K), isothermal process is assumed.

R: gas constant for air ( $\text{m}^2/\text{K}/\text{s}^2$ )

$A_s$ : slow valve cross sectional area ( $\text{m}^2$ )

$A_f$ : fast valve cross sectional area ( $\text{m}^2$ )

$F_f$ : friction force in CCA (N)

$\kappa$ : specific heat ratio (1.4 for air)

### 3.2.1 Clutch valve unit

An air tank provides the system with air at  $P_{airtank}$ . The four valves that control the air in- and outlet to the Clutch Concentric Actuator (CCA) are placed in the Clutch Valve Unit (CVU). This is a moulded metal component with complex air ducts that lead the air from the air supply tank to the CCA.

A principal sketch of a valve and how it is opened is depicted in Figure 3.2. A current,  $i$ , induces a magnetic field that moves (opens) the valve and enables air to flow through the opening with diameter  $D_{valve}$ . The current,  $i$ , is either high or low and controlled by the PWM-signals.

The input to the whole system subject to this study are the signals that control the air in- and outlet valves; the PWM-signals (**P**ulse-**W**idth-**M**odulation). By opening and closing the four air valves the pressure in the CCA is regu-

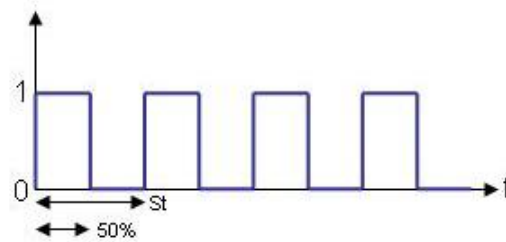


**Figure 3.3:** Principal sketch of a PWM signal set to 50 %.

lated and, thus the clutch position. A PWM-signal is a percentage figure. The percentage denotes how much of a given time period that the signal is high. For example, Figure 3.3 shows a 50 percent PWM-signal. In this application a high PWM-signal corresponds to an open, while a low signal corresponds to a closed valve.

There are four different PWM-signals. Two signals are used to disengage ( $s_d$ ,  $f_d$ ) and the other two to engage ( $s_e$ ,  $f_e$ ) the clutch. The subscripts  $d$  and  $e$  denote the signal type;  $d$  - disengage,  $e$  - engage. The other signal characterisation, namely the velocity of the engagement/disengagement, are denoted by  $s$  and  $f$  for slow and fast respectively. What differs the fast signals from the slow ones are the valves' physical design.

The "fast" valves have a larger diameter (3.7 [mm]) than the "slow" valves (2.7 [mm]) which enables a larger amount of air to pass through the former during a specific time period. Another characteristic of importance is that each valve is considered to be either open or closed. In other words you can not open the valve half way.

However, a specific PWM-signal in the form of a percentage figure, does not necessarily mean that the valve is fully open during that specific percentage of time. For example, it needs to be set on a higher value than 15 % to even open at all, and similarly there is no difference between the amount of air that flows through a valve set to be open between 80-100 %.

To sum up the valves behave due to two principles that at a first glance might appear as contradictory: the valves are either fully opened or completely closed but even so a certain opening time in percentage does not necessarily mean that the air flowing through the valve correspond to the mathematically calculated amount of air. Due to this a measurement of the valve behaviour must be included in the model.

The graph in Figure 3.4 show the difference between the real amount of air through the slow valve compared to the calculated amount. The measured flow is from a test performed on a slow valve where the normal litre per min [Nl/min], denoted  $Nl_{\text{min,slow}}$ , was measured for sonic flow at different PWM-signals i.e. maximum airflow through the valve. By transforming the normal

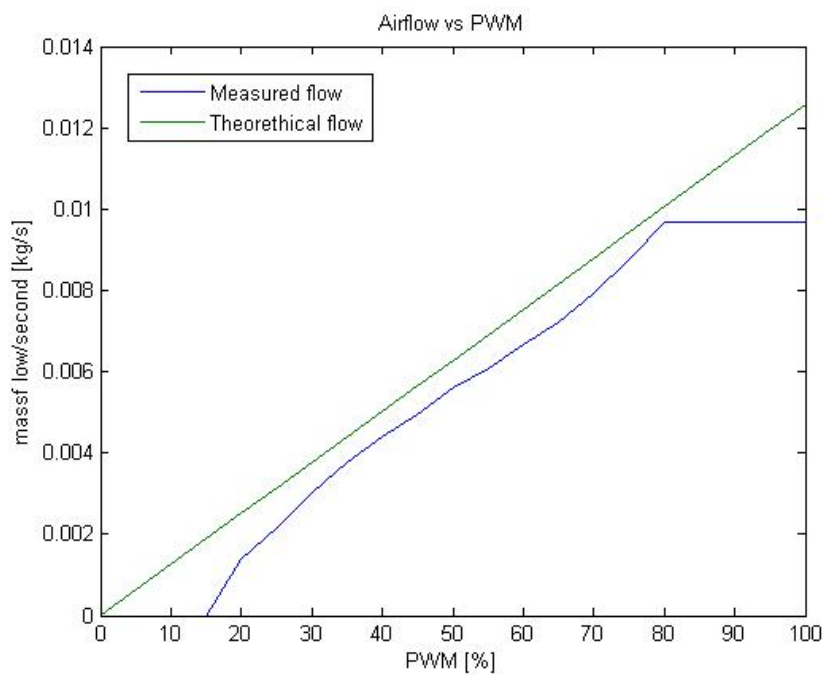


**Figure 3.4:** A graph where the phenomenon that there is a difference between the real amount of air ( $\dot{m}_{\text{real,slow}}$ ) compared to the calculated amount ( $\dot{m}_{\text{calc,slow}}$ ) that flows through a slow valve ( $\varnothing 2.7$  [mm]) is visible. The relation between these two graphs is the compensation factor  $C_{\text{cf,slow}}$  the model use to include the valve characteristics.

litre per min to the corresponding massflow per sec [kg/s], denoted  $\dot{\mathbf{m}}_{\text{real,slow}}$ , the model use the proportion, denoted  $\mathbf{C}_{\text{cf,slow}}$ , between these measured values for different PWM-signals and the theoretically calculated values for different PWM-signals, denoted  $\dot{\mathbf{m}}_{\text{calc,slow}}$ , see Eq. 3.1-3.2. By using this proportion as a compensation factor in the simulation the theoretical calculated mass airflow is scaled down. This compensation factor is also used for airflow through the valve when the flow no longer is sonic since the valve characteristic is assumed to stay the same. In the absence of measurements for the fast valve this valve is assumed to be acting like the slow valve, and through the assumption that the airflow is proportional to the valve area the valve characteristic can be related to a valve with a different area, see Eq. 3.3. Observe that  $\dot{\mathbf{m}}_{\text{calc,slow}}$  and  $\dot{\mathbf{m}}_{\text{calc,fast}}$  are vectors that contains the different mass flows for the different PWM-signals  $\in [0; 100]$  %. The computation of the compensation factors are carried out in an initializing script why the density  $\rho$  is the density of the air in the CCA from the beginning.

$$\dot{\mathbf{m}}_{\text{real,slow}} = \mathbf{N} \mathbf{I}_{\text{min,slow}} \frac{\rho^2 R T^2 0.001}{P_{\text{atm}} 273.15 \cdot 60} \quad (3.1)$$

$$\mathbf{C}_{\text{cf,slow}} = \frac{\dot{\mathbf{m}}_{\text{real,slow}}}{\dot{\mathbf{m}}_{\text{calc}}} \quad (3.2)$$

$$\dot{\mathbf{m}}_{\text{calc,fast}} = \frac{\dot{\mathbf{m}}_{\text{calc,slow}} A_{\text{fast}}}{A_{\text{slow}}} \quad (3.3)$$

### 3.2.2 Clutch Concentric Actuator

The Clutch Concentric Actuator is the compartment/space that is either filled or emptied with air. The increasing or decreasing air pressure in the CCA determines whether the throw-out bearing will move in either positive or negative x-direction, see Figure 3.6. For example, during a movement in positive x-direction, a disengagement movement, the force exerted on the throw-out bearing from the built up air pressure is larger than the sum of all forces working in the opposite direction. The largest force to overcome is the nonlinear force from the diaphragm spring.

### 3.2.3 Gas dynamics

As mentioned above the air in- and outlet is controlled by the valves in the Clutch Valve Unit (CVU). Since the driving force behind the movement of air in and out of the CCA is pressure difference between the, through the valves, combined air containing components (air supply tank, CCA, surroundings) this pressure difference needs to be taken into consideration. According to

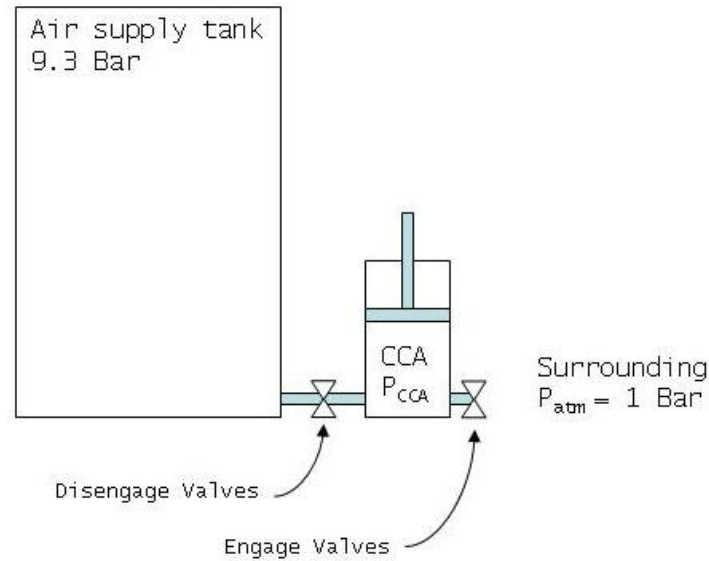


**Figure 3.5:** The simplification of the system from an air flow point of view.

[5] a pressure ratio of only 2:1 will cause the air flow to be sonic. As a consequence gas dynamics is of great importance for the analytical model. However, compressible flow theory is not trivial why analysis of this kind rarely end with a nice and neat algebraic equation.

To derive the equations for the throw-out bearing position the following assumptions are made:

- adiabatic flow conditions
- no impact from the kinetic energy due to flow movement
- the air is treated as an ideal gas

A simplification of the air flow system geometrically is to consider the valves to be the only thing that separates:

- (A) the Air supply tank and the CCA (disengage)
- (B) the CCA and the surrounding (engage)

This assumption is schematically depicted in Figure 3.5, where the nominal pressure in the Air supply tank and the atmospheric pressure surrounding the system is marked out.  $P_{CCA}$  will change as the valves are opened and closed.

In reality the different air compartments are combined through ducts with complex geometry. To set up an analytical model specific for these ducts

may be possible to some extent, but due to the same geometry there is a significant uncertainty for this type of analytical calculations [5]. For example the pressure loss caused by a  $90^\circ$  turn may vary between .3 to 1.4. In order to make realistic assumptions one may need to set up a test bench and study the air flow closely, but even so the difference from the simplified geometric approach used in this model may not be noticeable due to the much larger diameter in the ducts (10 mm) compared to the valve diameters (2.7 and 3.7 mm). It is thus reasonable to assume the CCA compartment to start on the other side of the valve as is shown in Figure 3.5. Even as the pressure is built up and the air flow eventually stops being sonic, this is still presumed to be a sound assumption since the duct volume is small compared to the CCA volume.

The last assumption for the equations including air flow is that the pressure in the CCA is immediately and simultaneously changed within the whole compartment as (i) air goes in or out and (ii) as the volume is changed when the piston moves. In reality the air density is probably higher at certain points in the CCA, for example close to the air inlet, and suddenly lowered close to the piston as it moves and increase the volume. However, the pressure differences are most likely very small in context to the whole pressure change and the assumption is thus considered to be motivated.

### 3.2.4 Air flow in and out of CCA

Since the same theory is applicable for outlet of air, the same equations are used. However it is important to keep track on how the subscripts suddenly denote different pressures, see Table 3.1.  $A$  is the cross sectional valve area (different if slow or fast valve),  $R$  is the universal gas constant and  $T$  the temperature.

	$P_{airtank}$	$P_{CCA}$	$P_{atm}$
Disengage	$p_2$	$p_1$	-
Engage	-	$p_2$	$p_1$

**Table 3.1:** How the subscripts in Eq 3.4-3.6 swich meaning depending on whether it is a disengaging or engaging movement.

Due to the large pressure differences that for the most part is present the air will start to flow as soon as any of the valves are opened. As long as the pressure difference is large enough, i.e. as long as the condition in Eq. 3.4 is true, the air flow will be *choked* which means it will flow through the valve with the maximum air flow calculated with Eq. 3.5 [5].



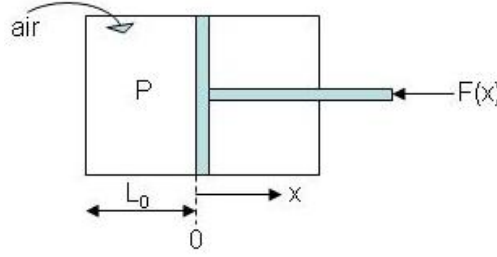


**Figure 3.6:** Movement  $x$  causing clutch disengagement.

$$\frac{p_1}{p_2} < \left( \frac{2}{\kappa + 1} \right)^{\kappa/(\kappa-1)} \approx 0.53 \quad (3.4)$$

$$\dot{m}_{max} = \sqrt{\kappa} \left( \frac{2}{\kappa + 1} \right)^{(1/2)(\kappa+1)/(\kappa-1)} \frac{p_2 A}{\sqrt{RT}} \quad (3.5)$$

When the air flow ceases being sonic, the air mass flow can be calculated with Eq. 3.6. It will eventually stop when both chambers have reached the same pressure.

$$\dot{m} = \frac{p_2 A}{\sqrt{RT}} \sqrt{\frac{2\kappa}{\kappa - 1} \left( \frac{p_1}{p_2} \right)^{2/\kappa} \left[ 1 - \left( \frac{p_1}{p_2} \right)^{\frac{\kappa-1}{\kappa}} \right]} \quad (3.6)$$

### 3.2.5 Piston movement

As seen in Figure 3.6, the movement causing a disengagement of the engine from the transmission is caused by movement  $x$  that in turn is caused by an increasing pressure  $P$  inside the CCA. As a starting point Newton's second law is set up for the sum of forces that act on the piston, Eq. 3.7.  $m_s$  in the equation is the mass of the parts that are moved i.e. the piston and the throw-out bearing. The different forces that are identified are the following (Eq. 3.8): the force caused by  $P_{CCA} - F_{CCA}$ , the force from the diaphragm spring -  $F(x)$ , the friction force caused by the friction between the edges of the piston and the cylinder wall -  $F_f$  and the force caused by the atmospheric air pressure from the surroundings -  $F_{atm}$ . The damping force,  $F_d$ , that always is present in one way or the other as soon as a spring is involved is not included in the model since nothing at all is known of this force. It is merely included in Eq. 3.8 to point out its probable existence.

The mass of the system,  $m_s$ , is merely guessed to be 4 [kg]. Also, little is known of the friction force exerted on the piston in the CCA. The maximum friction is 700 [N], and since this is the only known fact this value is used.

$$\sum F = m_s a = m_s \ddot{x} \quad (3.7)$$

$$\sum F = F_{CCA} - F(x) - F_f - F_{atm}(-F_d) \quad (3.8)$$

$F_{CCA}$  is the driving force caused by the built up pressure,  $P_{CCA}$  in the CCA. When modeling the pressure the perfect gas law is used, but instead of a fixed density,  $\rho$ , the density is dynamic due to the compression of air why it needs to be calculated in each time instant. In order to do so the total air mass in the cylinder has to be known as well as the total volume.

$$F_{CCA} = P_{CCA} A_{CCA} \quad (3.9)$$

$$P_{CCA} = \rho RT = \frac{m_{tot}}{V_{CCA}} RT \quad (3.10)$$

$$m_{tot} = m_0 + \int_0^t (\dot{m}_{in} - \dot{m}_{out}) dt \quad (3.11)$$

$$V = LA = (L_0 + x) A_{CCA} \quad (3.12)$$

Combining these equations (Eq. 3.10-3.9) gives the final expression for  $F_{CCA}$ , Eq. 3.13.

$$F_{CCA} = (m_0 + \int_0^t (\dot{m}_{in} - \dot{m}_{out}) dt) \frac{RT}{(L_0 + x)} \quad (3.13)$$

### 3.3 Part II - Force on Clutch plate

**Inputs:**

$x_{to}$ : throw-out bearing position (mm)

**Output:**

$F_{cp}$ : force on clutch plate from diaphragm spring (N)

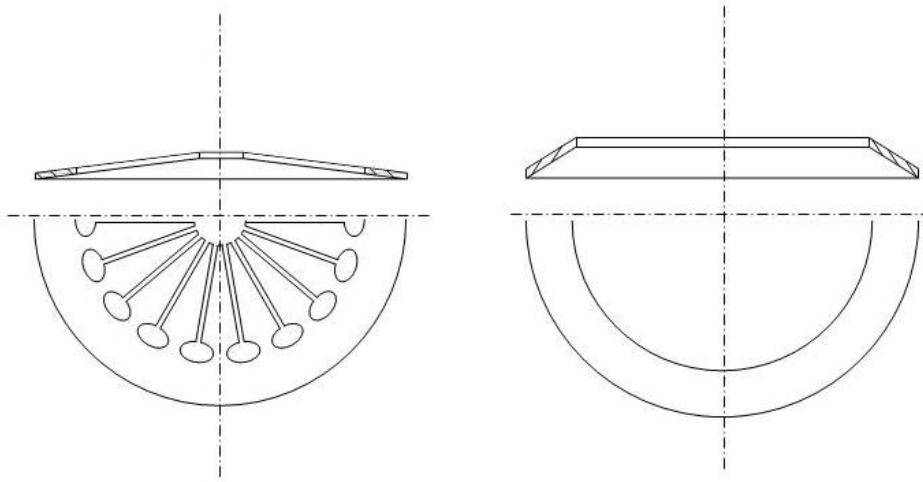


**Figure 3.7:** Diaphragm finger spring and clutch disk spring.

### 3.3.1 Diaphragm spring and Clutch plate

The spring with the greatest importance in the clutch is the diaphragm spring, see Figure 3.7. It can be viewed upon as a combination of an outer disk spring (right) and separate leaf springs (left). Leaf springs have a linear characteristic, while the outer solid disk spring behaves differently. It can be compared to an umbrella that in hard wind suddenly flips over.

When the throw-out bearing press against the fingers and force them in a certain direction the disk spring will suddenly flip and thus disconnect the clutch. The clutch plate itself, called the *flat spring*, also has an elastic effect in order to soften up the dis-/engage process to prevent unnecessarily large wear of the clutch. It is well known that the clutch age with usage. What really happens is that the diaphragm spring gets worn out; imagine an old umbrella that has lost its stiffness.

Due to the springs nonlinear characteristic it is included in the model through *measured data* provided by the supplier of the diaphragm spring. In figure 3.8 both the force  $F(x)$  acting on the throw-out bearing and the force on the clutch plate  $F_{cp}$  is plotted. Logically  $F_{cp}$  decreases as  $F(x)$  increases and vice versa. If the flat spring in the clutch plate would be excluded the  $F(x)$  graph has a sharper "knee" before it bends off horizontally, and thus the transition from disengaged to engaged clutch occur more abruptly. It is also clear that the diaphragm spring is affected by hysteresis. However the model is built in a simplified manner excluding this fact only using the upper plotted data. This means that the diaphragm spring in the model is acting as if the position  $x_{to}$  always is reached after a movement in positive x-direction.

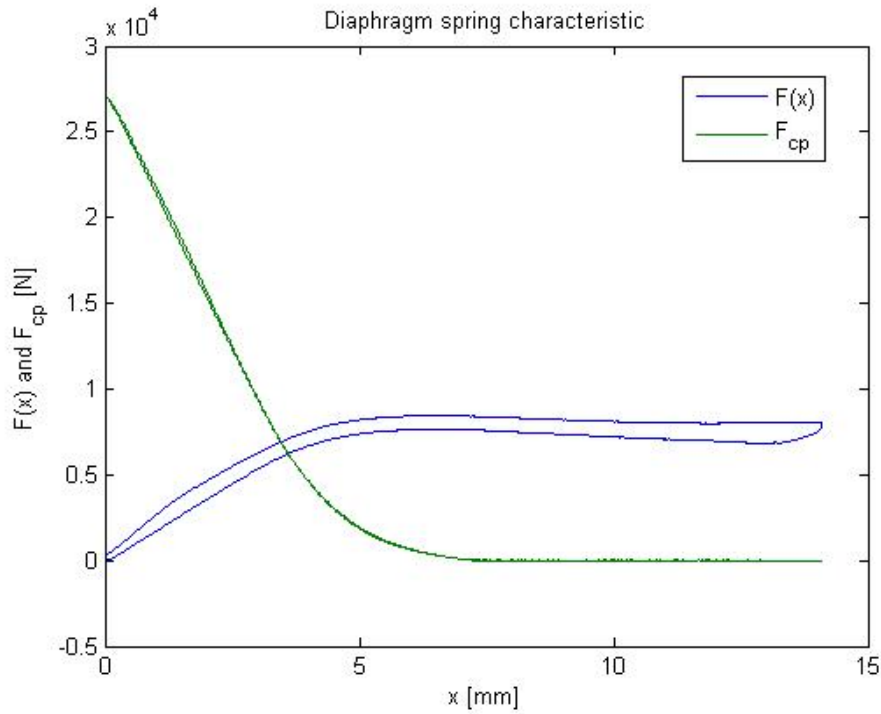


Figure 3.8:  $F(x)$  and  $F_{cp}$  .

$$F_{cp} = F_{cp}(x) \quad (3.14)$$

### 3.4 Part III - Transferred torque

**Inputs:**

$F_{cp}$ : force on clutch plate from diaphragm spring (N)

**Output:**

$T_{gbx}$ : transmitted torque to gear box input shaft (Nm)

**Constants:**

$R_i$ : inner radius of clutch plate (m)

$R_o$ : outer radius of clutch plate (m)

$\mu$ : friction coefficient, clutch plate

#### 3.4.1 Friction, radius and wear

As stated above in section 3.1 there are several parameters and characteristics that effect how much torque that is transmitted to the gearbox. In Part III

the friction coefficient on the clutch plate surface, the wear of the clutch and the inner and outer radius are identified parameters of importance. For this model the fact that the clutch in principal works the same as disc breaks are exploited. Equations from [4] are incorporated and give the maximum transferrable torque to the gearbox.

Two outputs are provided by the model, one for a new (Eq. 3.15) and the other for a run in clutch plate (Eq. 3.16). The constants used are chosen according to the hardware component owner at Volvo Powertrain. The friction coefficient,  $\mu$ , on clutch plate surface may vary between [.27-.47]. Value used for the validation test is .3. The magnitudes of inner and outer clutch plate radius are set to 260 and 430 [mm] respectively.

$$T_{gbx} = \frac{2\mu(R_o^3 - R_i^3)}{3(R_o^2 - R_i^2)} F_{cp} \quad (3.15)$$

$$T_{gbx} = \mu F_{cp} \frac{R_o + R_i}{2} \quad (3.16)$$

### 3.5 Formulation of the complete model

In the above sections all physical and mathematical relations that are needed for a clutch model are derived. Here follows a summary of all the equations that will give a better overview of the whole system. A sketch of the complete system and how it is put together can be seen in Figure 3.9. Specifically observe how the compensation factors  $C_{cf,fast}$  and  $C_{cf,slow}$  for the valve characteristics are included in Eq. 3.21 and Eq. 3.23.

#### Equations for Part I:

$$m_s \ddot{x} = F_{CCA}(m_{tot}, x) - F(x) - F_f - F_{atm} \quad (3.17)$$

$$F_{CCA}(m_{tot}, x) = \frac{m_{tot} RT}{L_0 + x} \quad (3.18)$$

$$m_{tot} = m_0 + \int_0^t (\dot{m}_{in,tot} - \dot{m}_{out,tot}) dt \quad (3.19)$$

$$\dot{m}_{in} = \begin{cases} \sqrt{\kappa} \left( \frac{2}{\kappa+1} \right)^{(1/2)(\kappa+1)/(\kappa-1)} \frac{P_{airtank} A}{\sqrt{RT}} & ; \text{if } \frac{P_{CCA}}{P_{airtank}} \lesssim 0.5283 \\ \frac{P_{CCA} A}{\sqrt{RT}} \sqrt{\frac{2\kappa}{\kappa-1} \left( \frac{P_{airtank}}{P_{CCA}} \right)^{2/\kappa} \left[ 1 - \left( \frac{P_{airtank}}{P_{CCA}} \right)^{\frac{\kappa-1}{\kappa}} \right]} & ; \text{else} \end{cases} \quad (3.20)$$

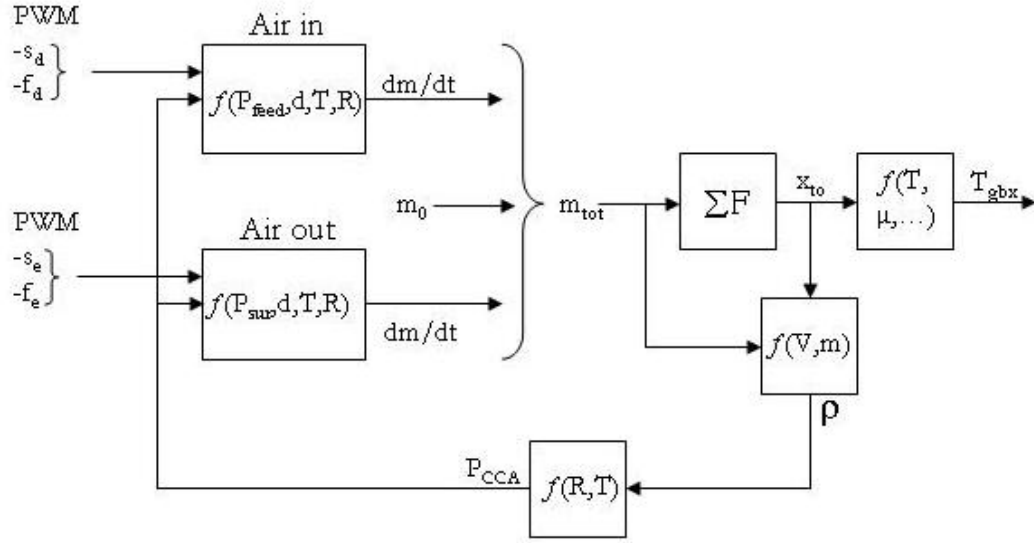


**Figure 3.9:** A flow chart that show how the clutch system in theory is put together, first analytically and later in Simulink.

$$\dot{m}_{in,tot} = \dot{m}_{in}(s_d) \cdot \mathbf{C}_{cf,slow}(s_d) + \dot{m}_{in}(f_d) \cdot \mathbf{C}_{cf,fast}(f_d) \quad (3.21)$$

$$\dot{m}_{out} = \begin{cases} \sqrt{\kappa} \left( \frac{2}{\kappa+1} \right)^{(1/2)(\kappa+1)/(\kappa-1)} \frac{P_{CCA} A}{\sqrt{RT}} & ; \text{if } \frac{P_{atm}}{P_{CCA}} \lesssim 0.5283 \\ \frac{P_{atm} A}{\sqrt{RT}} \sqrt{\frac{2\kappa}{\kappa-1}} \left( \frac{P_{CCA}}{P_{atm}} \right)^{2/\kappa} \left[ 1 - \left( \frac{P_{CCA}}{P_{atm}} \right)^{\frac{\kappa-1}{\kappa}} \right] & ; \text{else} \end{cases} \quad (3.22)$$

$$\dot{m}_{out,tot} = \dot{m}_{out}(s_e) \cdot \mathbf{C}_{cf,slow}(s_e) + \dot{m}_{out}(f_e) \cdot \mathbf{C}_{cf,fast}(f_e) \quad (3.23)$$

$$P_{CCA} = \rho RT = \frac{m_{tot}}{V_{CCA}} RT \quad (3.24)$$

$$V_{CCA} = (L_0 + x) A_{CCA} \quad (3.25)$$

**Equations for Part II:**

$$F_{cp} = F_{cp}(x) \quad (3.26)$$

**Equations for Part III:**

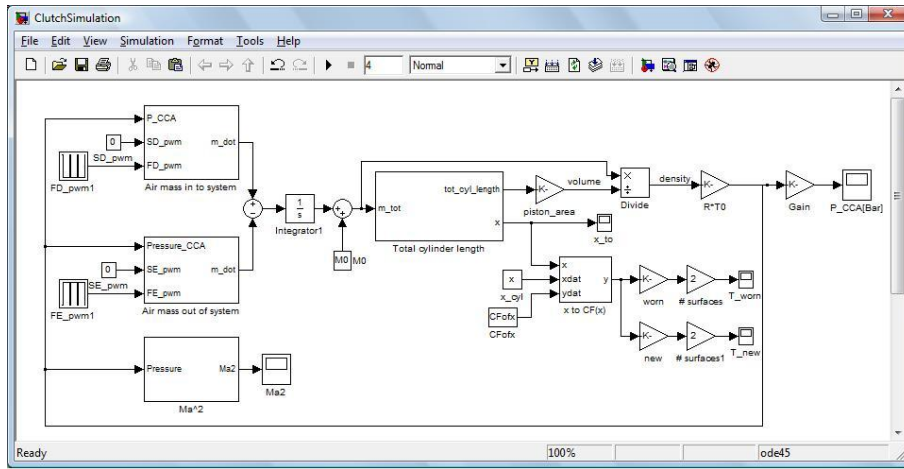
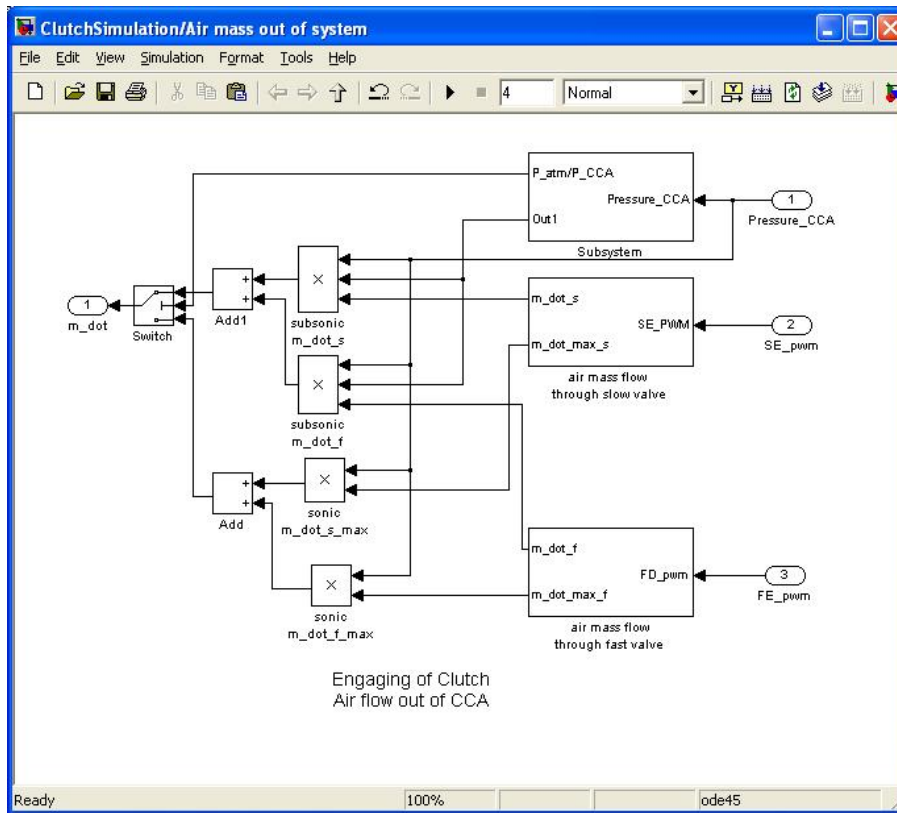


Figure 3.10: The simulation core.

$$T_{gbx} = T_{gbx}(F_{cp}) = \begin{cases} \frac{2\mu(R_o^3 - R_i^3)}{3(R_o^2 - R_i^2)} F_{cp} & ; \text{new clutch plate} \\ \mu F_{cp} \frac{R_o + R_i}{2} & ; \text{old clutch plate} \end{cases} \quad (3.27)$$

### 3.6 Simulation Model

The analytical model derived above is implemented in MATLAB-Simulink. In fact, the analytical model has been revised throughout the process according to stated method, [3]. Figure 3.9 is an attempt to illustrate how the model fundamentally is constructed. Figure 3.10-3.12 is simply screen shots of how the schematic flow chart in Figure 3.9 is transformed to MATLAB-Simulink. An initializing MATLAB script sets all parameters of interest and this is also where it is possible to change parameters subject to study. The diaphragm spring data as well as the flat spring data is incorporated in the model through look-up tables.



**Figure 3.11:** Subsystem where the amount of air that goes out of the CCA is calculated depending on the PWM-signals that control the disengage valves.

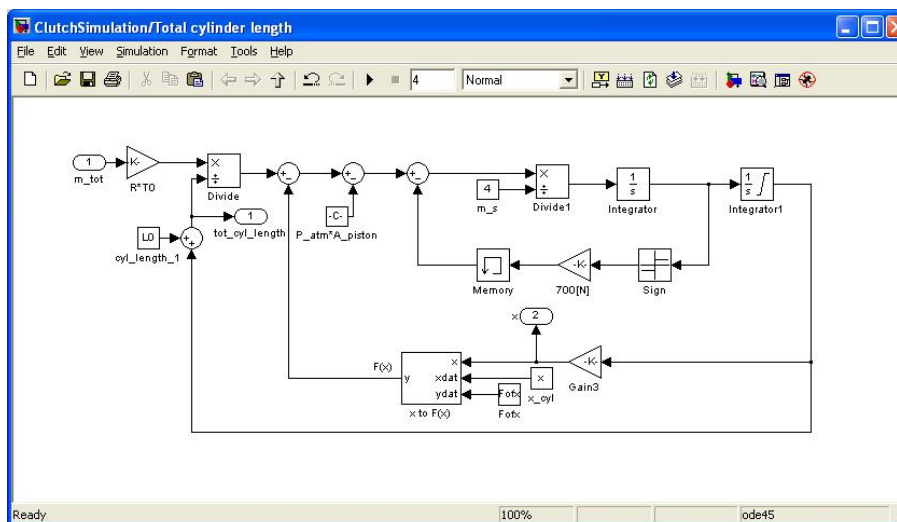


**Figure 3.12:** Subsystem where the translational movement  $x_{to}$  is calculated, as well as the total length of the CCA. The length is crucial to calculate the CCA-volume which is needed in order to decide the air density.



# 4

## Results

To verify the quality of an analytically formulated physical model the importance of real data is given [3]. There are three different sets of accessible data:

1. Valve tests. Two tests carried out during 2007 in test bench, where disengagement time was measured as the two disengagement valves were given a 100 % PWM-signal. The test shows how long time that elapsed from activation until the CCA had traveled 13 mm. Pressure difference: 8 [Bar].
2. Disengagement and engagement time at different PWM-signals. Test in vehicle where signals were logged (2011-01-26), and results later analyzed in Matlab. Truck placed in a garage, thus  $T \approx 20^\circ$  C. Pressure difference: 7 [Bar].
3. Test data from a drive line rig with torque sensor mounted on gearbox shaft.

The model contains several parameters of different importance to the simulation result. Some of them are possible to assign more or less certain values to (e.g.  $P_{airtank}$ ,  $A_{CCA}$ ,  $A_s$ ,  $A_f$ ) while others are simply estimated (e.g.  $m_s$ ,  $F_f$ ,  $\mu$ ). This may of course affect the outcome. But before the comparisons with data starts it is suitable to verify that the simulation model behaves as expected.

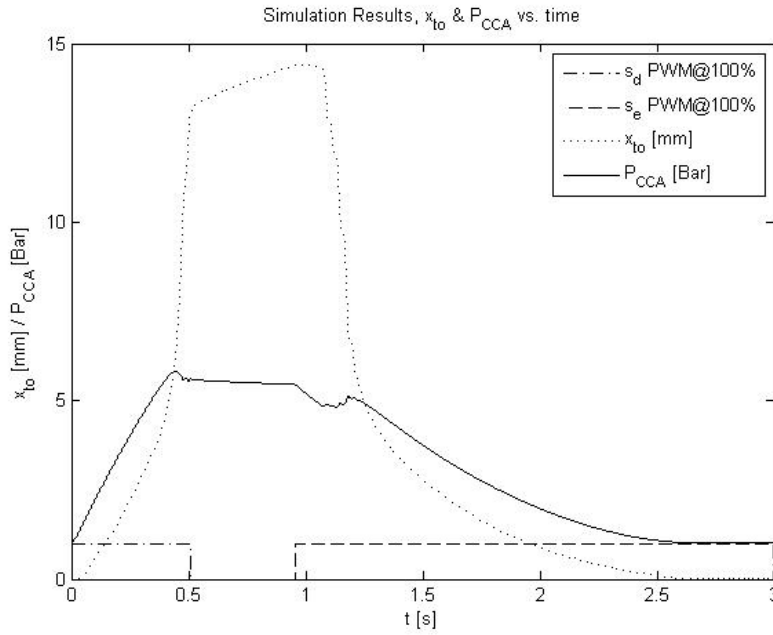


**Figure 4.1:** Simulation model behaviour due to PWM-signals. As  $x_{to}$  increases the pressure  $P_{CCA}$  increases and vice versa.

## 4.1 Model behavior

The test to illuminate the mere model function is simply a disengagement PWM-signal ( $s_d(100\%)$ ) followed by an engagement PWM-signal ( $s_e(100\%)$ ). The graphs in Figure 4.1-4.2 shows the throw-out bearing position  $x_{to}$ ; the CCA pressure and; the torque transferred to the gearbox from the same test setup.

Figure 4.3 illustrates how the amount of air that flows into the system depends on the pressure difference between air supply tank and the built up pressure in CCA. During this test sequence the disengaging PWM-signal  $s_d$  were held at a constant 100% throughout the test.

## 4.2 Valve tests in test bench

There are two sets of test results available from valve component tests. One is from a test with the objective to compare the performance of two different types of valves [2] but with the same cross sectional area. The other test was performed in order to see the difference, if any, in disengagement time with reduced amount of copper in the CVU coils [1]. There are a slight difference in the results from the tests why the shortest and longest measured elapsed

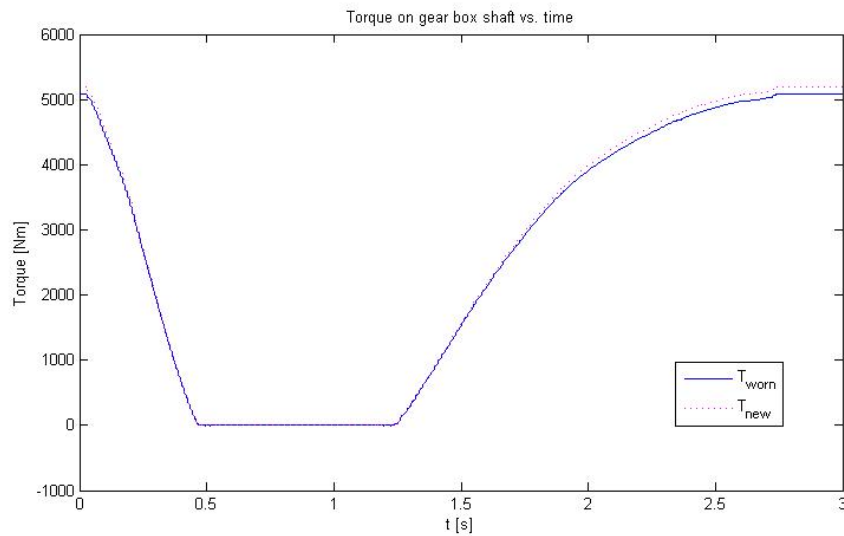


Figure 4.2: The torque transferred due to movement  $x_{to}$ . (Simulation)

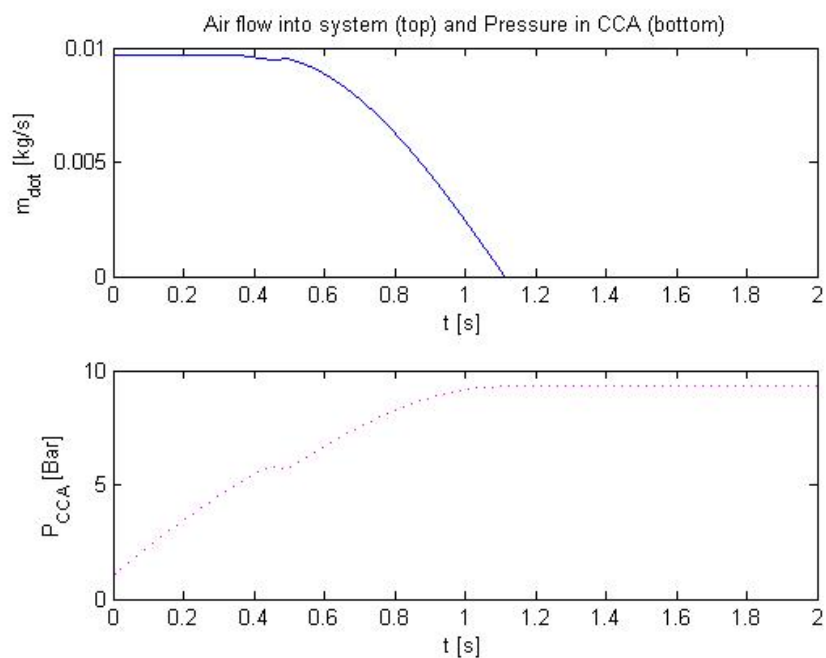


Figure 4.3: Air flow and pressure during constant  $s_d$  PWM-signal at 100%. (Simulation)

time periods are accounted for in Table 4.1. The results from the simulated model are shown in the same table.

**Table 4.1:** Valve test in test bench, T @  $\approx 20^\circ\text{C}$ , P 8 Bar, travel 13 mm.

Valve	$t[\text{s}]$ , test bench	$t[\text{s}]$ , sim.model	diff. (min-max)
$s_d$	0.47-0.52	0.52-0.53	0-0.06
$f_d$	0.31-0.35	0.29	0.02-0.06
$s_d$ and $f_d$	0.23-0.28	0.18	0.05-0.1

### 4.3 In vehicle test

The test took place in January 2011 at AB Volvo, Lundby. A computer was hooked up to the Transmission Electrical Control Unit - the TECU. Through the computer it is possible to control, among others, the PWM-signals, while logging for example the throw out bearing position,  $x_{to}$ . When the disengaging PWM-signals are given a value the clutch will do a full disengagement movement, that is  $\approx 18[\text{mm}]$ . In reality the movement is never more than  $13[\text{mm}]$ , during a shift for example, since a full disengagement is particularly harmful to the clutch. In a non mannered situation this only occurs during a so called limp-home situation. That is in the case of problem or break down when the driver must be certain that the gear box really is detached from the engine. Back to the test set up. Several different percentage figures were tested for both engage and disengage movement. The same figures were later run in the simulation model. See Table 4.2 and 4.3 for the results. It is important that the simulation test is set up accordingly as the vehicle test. Due to the lack of a pressure sensor in the CCA the disengagement valves were held open during a long enough time period that could ensure that the CCA-pressure reached the same level as the feed pressure, in this case 8 [Bar].

**Table 4.2:** In vehicle test, T @  $\approx 20^\circ\text{C}$ , P 8[Bar], travel  $\approx 18[\text{mm}]$ .

Valve	PWM-%	Diseng. $t[\text{s}]$ , vehicle	Diseng. $t[\text{s}]$ , sim.model
$s_d$	100	1.0	0.6
$s_d$	90	1.0	0.6
$s_d$	70	1.1	0.75
$s_d$	40	1.7	1.35
$s_d$	30	2.7	2.0
$f_d$	100	0.7	0.32
$f_d$	90	0.7	0.32
$f_d$	70	0.9	0.4
$f_d$	40	1.6	0.7
$f_d$	30	3.0	1.0

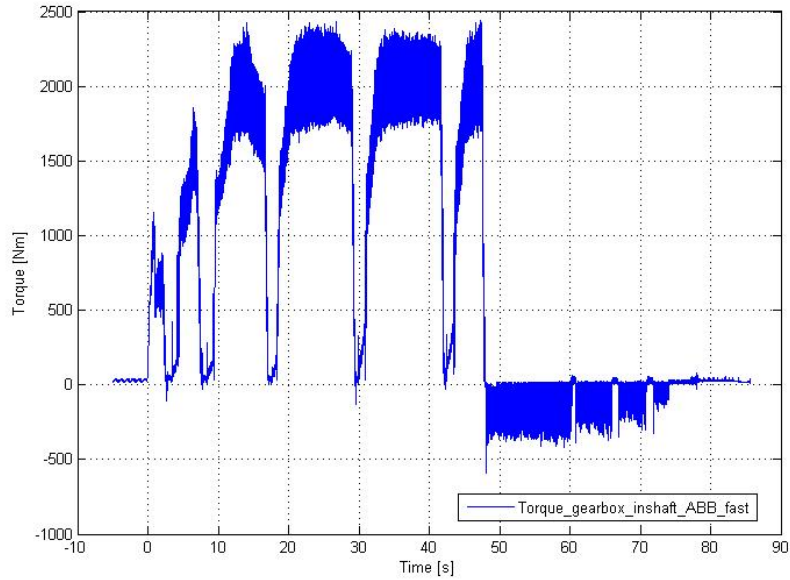


**Figure 4.4:** Test results from a drive line test rig where the torque on the gear box input shaft is plotted.

## 4.4 Drive line rig test

The test was carried out in June 2010 in one of the test rigs at AB Volvo, Lundby, see Figure 4.4. Even if the results are difficult to relate to the model at present concerning the shape of the plot, it is at least possible to see that the magnitude of the torque transferred during this test to the gear box input shaft was about 2500 [Nm].

**Table 4.3:** In vehicle test, T @  $\approx 20^{\circ}\text{C}$ , travel  $\approx 18[\text{mm}]$ .

Valve	PWM-%	Eng. $t[\text{s}]$ , vehicle P in CCA $\approx 8[\text{Bar}]$	Eng. $t[\text{s}]$ , sim.model P in CCA $8[\text{Bar}]$
$s_e$	100	3.1	2.1
$s_e$	60	3.8	3
$s_e$	40	5.3	4.4
$s_e$	20	-	-
$f_e$	100	1.9	1.3
$f_e$	60	2.35	1.7
$f_e$	40	3.55	2.44
$f_e$	20	No movement	-



# 5

## Discussion and conclusions

The results presented in chapter 4 will now be analysed and discussed.

Let's start with the results in section 4.1. The model appears to behave as somewhat expected. The throw-out bearing position,  $x_{to}$ , increases as  $s_d$  is high, i.e. the slow disengagement valve is open and letting air into the system (Figure 4.1). Slowly at first and then, as the CCA-pressure is built up, the contrary forces from friction and spring are overwon. The pressure rises as the air mass in the CCA increases even if the CCA-volume also increases with the axial movement. One can also observe what happens when the  $s_d$  valve is shut.  $x_{to}$  continues to increase even as no air is flowing into the system, while the CCA-pressure decreases. This may be explained by the fact that the movement  $x_{to}$  is ongoing when the addition of air is suddenly turned off. The density of the air in the CCA is recalculated and thus, the pressure will decrease. When the  $s_e$  valve now is opened the air will start to flow out of the CCA. The air-flow is from the beginning sonic, but slows down as the pressure in the CCA decrease. The returning movement,  $-x_{to}$ , will however linger a while due to the continuously lower air density. The torque transferred to the gear box shaft is calculated under two different assumptions. The first one is that the lamelles are new, and the other is that they are worn in, Figure 4.2. The torque decreases with increasing  $x_{to}$  and increases as  $x_{to}$  returns to initial position.

As already mentioned, the data available from experimental tests are important to the validation process. When comparing the results from test runs, both experimental and simulated, the aim is naturally to obtain a small difference, figure 5.1 [3]. However, "small" is a word representing a quantity of unknown dimension that for different models can be of different magnitude.

The first part of the model as stated in 3.1 is from PWM-signal to  $x_{to}$ . In order to see how the model corresponds to reality both the results from the

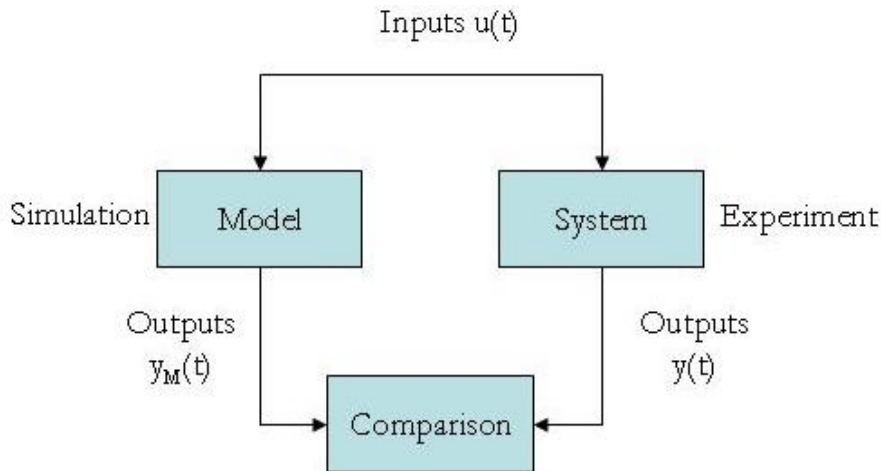


**Figure 5.1:** An illustration of what [3] entitle as a validity test.

valve tests in test bench (Section 4.2) and the in vehicle test (Section 4.3) are used. The valve test results presented in Table 4.1 are considered satisfactory. There is a slight difference between the test results and the simulation results, but to end up with the exact same result is not particularly realistic due to all the assumptions made in order to set up the analytical model for the air flow. However, one should be observing that the simulated results differs from the test results in opposite ways. The simulated time measured for  $s_d$  is slightly *larger* than the time measured in the experiment, while the simulated time for a  $f_d$  signal is slightly *less* than the time in the experiment.

The difference in measured elapse time for the case when both valves are opened is also larger. This may have to do with the Clutch Valve Unit design. The model does not take into account for example that the pressure in the CVU ducts may effect the air flow, nor any turbulence. Here one must be aware of the fact that in reality this is a situation with compressible flow and naturally assumptions that make it possible to derive algebraic equations may affect the end result. Even if the nonlinear valve characteristics that is described in 3.2.1 is included in the model this might not be enough in case the flow through one valve is effected by weather the other valve is held open as well.

Other sources of error may be that the temperature is not known for certain. The test experiment were carried out in a test bench placed indoors why the temperature in the model were estimated to  $20^{\circ}C$ . This would not effect the outcome very much, but is still worth mentioning.

In the in vehicle test different PWM-percentages were tested. When comparing the disengagement time for the slow valve,  $s_d$ , from the in vehicle test and the simulation model there is a clear difference, Table 4.2. The difference



in time also appears to increase as the PWM-signal percentage is decreased. An interesting observation when comparing the test results is however that the disengagement time is *longer* for the  $f_d(30\%)$  signal than for  $s_d(30\%)$ . The expected test result, in theory, is naturally the opposite since a larger valve diameter implies more air flow and thus a shorter disengagement time. The results from the disengagement test indicates the same thing; even if the recording of the  $s_e(20\%)$  test was unsuccessful, it did cause a movement of the clutch, however when  $f_e(20\%)$  was tested nothing happened. An explanation to this behaviour could be that the assumption presented in section 3.2.1, that the valve characteristics for the fast valve is the same as the slow valve, may be wrong. Therefore it might be necessary to perform the same tests on the fast valve ( $\varnothing 3.7$  [mm]) where one measures the airflow vs. PWM-percentage, as presented for the slow valve in Figure 3.4.

When comparing the disengagement results in Table 4.3 one can conclude that they may not be good enough but at least they are in the correct order of magnitude. With the detected possible behavioral difference between the slow and fast valves taken into account the result may supposedly be better with fast valve characteristics certified and included.

The results from the in vehicle test can also be used to conduct another verification, namely the results from the valve tests in the test bench. As it turns out the time it takes for the CCA movement to reach 13[mm] in the in vehicle test is longer than the bench mark test imply. For  $s_d(100\%)$  it takes 0.75 [s] compared to the valve test bench result 0.47-0.52 [s]. For a similar comparison the  $f_d(100\%)$  needs 0.52 [s] compared to 0.31-0.35 [s] in the valve test bench. This may indicate that the valves' movement pattern or the behavior of the system as a whole is different than when each component is individually tested. It is however known that the real truck needs three sample periods to react compared to none in the test bench and simulation. One sample period is 20 ms which would diminish the difference with 0.06 s. Even so there is a substantial difference between the test results.

Through Part II and III, the predicted end station for this thesis, the torque transferred to the gear box input shaft, is reached. It is important to observe that the graph in Figure 4.2 show the maximum transferrable torque in comparison to Figure 4.4 that show results from a test where the in reality transferred torque was measured. Due to this there is naturally a difference in torque magnitude in the figures. However, some improvements of the model could be beneficial. For example, no energy losses are included such as heat generation while the clutch pad slips during an engagement process.

Figure 4.2 shows the simulated results from both a new and a worn in lamell. There is a slight difference between the magnitude of the transferred torque, but since other simplifications and assumptions present in the model may have a larger impact on the result the uncertainty in the outcome may indicate that it won't matter which analytical model one chooses. Therefore, if the clutch

wear is to be studied with the model this might not be the proper way to include it.

## 5.1 Uncertainties

Quantities present in the model that are not known for certain are e.g.:

- The mass  $m_s$  in equation 3.7 describing the  $x_{to}$ -movement is unknown.
- The friction coefficient for the lamell may vary in the interval [.27-.47].
- The characteristic of the friction force in the CCA.

Another significant source of error in the comparison between the model and, for example, the in vehicle test results is that there is limited knowledge of if the diaphragm spring and CCA are exactly the same as the modeled ones in the simulation. This would of course effect the outcome and a comparison between the results would not be realistic.

## 5.2 Final conclusions

To begin with, the model behaves conceptually as expected. An inlet of air  $\dot{m}_{in}$  causes a translational movement  $x_{to}$  that in turn causes a interruption of torque transfer to the gear box, and vice versa. The simulated translational movement  $x_{to}$  caused by air inlet through the  $s_d$ -valve corresponds fairly well to test results. However, air inlet through the fast valve needs further investigation. The same tests conducted on the slow valve to see the valve characteristics would be beneficial to have for the fast valve as well.

The magnitude of the transferred torque is hard to analyse with the existing data. More tests with the purpose to study the torque on the gearbox input shaft would be necessary to decide whether the model need more development before an implementation.

The question that has arisen is: Is it beneficial to replace the empirical models that are used in the transmission function tests at present? The for this thesis developed analytical model aimed at the exclusion of as much measured data as possible; however there are certain components that are too complex in its function to apply a mathematical expression. For example, the nonlinear diaphragm spring is included in the model through measurement data. On the other hand, it is far more simple to generate test data from *one or two*

---

*components* (the diaphragm spring, the valve characteristics) in comparison to a complete clutch concept why the usage of the analytical model can be emphasized as beneficial.

All in all, the most important benefit that the thesis contributes to might be the enlarged apprehension of the clutch function in theory. For even though the theory does not obtain exact applicable results for function simulations at this state, it might do so in an extended version in the future.



# 6

## Future work

In case it is found beneficial enough to continue to strive towards a pure analytical clutch model, further model development and test generation is necessary. If it turns out that an update through test data specific for fast valve characteristics is enough to obtain more realistic air in and outlet behaviour through the fast valve, main focus should be the investigation of what goes on at the clutch disk. That is, to examine what force is exerted on the lamell from the diaphragm spring, and how much of that force is *really* transferred to the lamell. This may require some sort of test setup where tests can be performed during close observations and little disturbances.

When a model is obtained that behaves satisfactory it will off course need to be discretised. This was included in the scope for this thesis from the beginning but has not been prioritized. It appeared far more important to end up with a model that behaved as realistically as possible.



# Bibliography

- [1] Measurement of disengagement time, less copper. Engineering Report, October 2007.
- [2] Measurement of disengagement time, valve types. Engineering Report, May 2007.
- [3] Lennart Ljung and Torkel Glad. *Modeling of Dynamic Systems*. Prentice Hall, Upper Saddle River, NJ, 2002.
- [4] Mart Mägi and Kjell Melkersson. *Lärobok i Maskinelement*. EcoDev International AB, Gothenburg, 2007.
- [5] Frank M. White. *Fluid Mechanics*. McGraw-Hill, New York, New York, 2008.